The perception of ego-motion change in environments with varying depth: Interaction of stereo and optic flow

Florian Ott Department of Biology, University of Tübingen, Tübingen, Germany

Ladina Pohl Department of Biology, University of Tübingen, Tübingen, Germany

Marc Halfmann Department of Biology, University of Tübingen, Tübingen, Germany

Gregor Hardiess Department of Biology, University of Tübingen, Tübingen, Germany

Hanspeter A. Mallot Department of Biology, University of Tübingen, Tübingen, Germany

When estimating ego-motion in environments (e.g., tunnels, streets) with varying depth, human subjects confuse ego-acceleration with environment narrowing and ego-deceleration with environment widening. Festl, Recktenwald, Yuan, and Mallot (2012) demonstrated that in nonstereoscopic viewing conditions, this happens despite the fact that retinal measurements of acceleration rate—a variable related to tau-dot—should allow veridical perception. Here we address the question of whether additional depth cues (specifically binocular stereo, object occlusion, or constant average object size) help break the confusion between narrowing and acceleration. Using a forced-choice paradigm, the confusion is shown to persist even if unambiguous stereo information is provided. The confusion can also be demonstrated in an adjustment task in which subjects were asked to keep a constant speed in a tunnel with varying diameter: Subjects increased speed in widening sections and decreased speed in narrowing sections even though stereoscopic depth information was provided. If object-based depth information (stereo, occlusion, constant average object size) is added, the confusion between narrowing and acceleration still remains but may be slightly reduced. All experiments are consistent with a simple matched filter algorithm for ego-motion detection, neglecting both parallactic and stereoscopic depth information, but leave open the possibility of cue combination at a later stage.

Introduction

In the analysis of optic flow, the estimation of ego-motion and the estimation of the environmental depth pattern (structure from motion) are two intrinsically related tasks. This is obvious for the well-known depth–velocity ambiguity—that is, the fact that optic flow does not allow one to recover the speed of translational ego-motion or the scale of environmental depth but rather only their ratio. This ambiguity is usually accounted for by treating translation as a unit vector ("heading") and considering the environment only in the form of relative depth (i.e., the ratio of depth and ego-motion speed). Still, the contribution of optic flow to the perception of vection, or ego-motion speed, is well established (e.g., Berthoz, Pavard, & Young, 1975; Dichgans & Brandt, 1978; Mohler, Thompson, Creem-Regehr, Pick, & Warren, 2007; Palmisano, Allison, Schira, & Barry, 2015).

In principle, the depth–velocity ambiguity can be overcome by independent assessments of depth (visually; e.g., from stereopsis) or ego-motion (e.g., from vestibular cues). Indeed, integration of visual and vestibular cues has been shown to play an important role both in the judgment of heading (e.g., Gu, Watkins, Angelaki, & DeAngelis, 2006) and in the estimation of traveled distance (Harris, Jenkin, & Zikovitz, 2000). Here, however, we focus on the

Citation: Ott, F., Pohl, L., Halfmann, M., Hardiess, G., & Mallot, H. A. (2016). The perception of ego-motion change in environments with varying depth: Interaction of stereo and optic flow. *Journal of Vision, 16*(9):4, 1–15, doi:10.1167/16.9.4.

doi: 10.1167/16.9.4 Received September 29, 2015; published July 21, 2016 ISSN 1534-7362

possible contributions of visual cues. The classic approach to ego-motion detection from optic flow is based on the projection equation for moving patterns (Bruss & Horn, 1983; Koenderink & van Doorn, 1987; Longuet-Higgins & Prazdny, 1980) or the epipolar line constraint in discretized ego-motion models (Longuet-Higgins, 1981; for a review see Raudies & Neumann, 2012). In most algorithms, relative depth on the one hand and the ego-motion parameters of translation and rotation on the other are estimated in a joint process. Therefore, independent cues to environmental structure can be used to improve the result, as is indeed demonstrated in numerical simulations by Raudies and Neumann (2012). Other algorithms, such as the local discontinuity approach by Rieger and Lawton (1985), the subspace approaches by Heeger and Jepson (1992) and Lappe and Rauschecker (1994), or the template-matching algorithms by Franz, Chahl, and Krapp (2004) and Perrone and Stone (1994), compute heading and rotation independent of relative depth. As models of human ego-motion detection, these models predict that independent depth information should be of little help in ego-motion estimates.

Empirical evidence for the use of visual depth cues in ego-motion estimation has been collected for various ego-motion-related percepts. For example, van den Berg and Brenner (1994) found that heading judgments when moving through a cloud of dots become less sensitive to noise when stereo cues are added. Because the gradual change of stereo disparity resulting from the simulated approach to the targets (dots) in the optic flow display did not affect this finding, the authors concluded that stereo disparity is used only for inferring depth order, not quantitative depth. Ehrlich, Beck, Crowell, Freeman, and Banks (1998) presented optic flow patterns of simulated gaze rotations and found that curved ego-motion trajectories are erroneously perceived. Adding stereo information does not resolve this misperception. Butler, Campos, Bülthoff, and Smith (2011) demonstrated that adding stereo information in a visual–vestibular integration scheme for heading leads to an improved cue combination compared with nonstereoscopic stimulation.

The role of perceived depth in perceived ego-motion speed was studied by Wist, Diener, Dichgans, and Brandt (1975) for the case of cyclovection induced by a rotating striped drum pattern. Perceived depth was modulated by putting a neutral filter in front of one eye; this is known to induce a time lag in the perception of a passing intensity edge, which together with the object motion produces an interocular disparity (Pulfrich effect). The perceived angular ego-motion speed was found to increase if larger stereoscopic depth was simulated, which is surprising given the fact that rotational optic flow does not depend on depth at all. The authors suggested that the cyclovection percept is generated indirectly, using the local translation pattern in different parts of the visual field, which in turn might be affected by perceived depth. More recently, Palmisano (1996, 2002) studied the effect of stereo information on the onset and duration of the qualitative sense of vection irrespective of the quantitative perceived speed. His findings suggest that the sense of vection is strengthened by stereoscopic information—not by way of disambiguating optic flow and environmental depth, but rather by feeding an additional channel for motion in depth, which independently supports the sense of vection. Similarly, perceived ego-motion speed from video clips of car driving is higher if the clips are stereoscopically presented (Brooks & Rafat, 2015).

Gray and Regan (1998) investigated the role of stereoscopic disparities and image expansion in the perception of time to collision and found that accuracy and discrimination are best if both cues are available. However, performance in the single-cue experiments may have been affected by cue conflict because the "monocular only" stimulus was actually viewed binocularly on a single monitor (i.e., with disparity zero), whereas in the "binocular only" experiment, optic flow would signal zero ego-motion. This cue-conflict situation was studied in more detail by Howard, Fujii, and Allison (2014), who concluded that the cues dissociate rather than combine.

Taken together, the experimental evidence indicates that the interaction of stereo and optic flow is not realized by combining pointwise depth and image flow data in an early vision ego-motion algorithm, but rather on a later state of visual processing. It may thus be considered a case of weak or late integration in the sense that initial processing occurs separately for the two cues, whereas combinations occur only after this initial processing. The joint representation supporting the combination of independently obtained depth and ego-motion data requires a spatial working memory that may be related to other such working memories suggested for a variety of related spatiotemporal tasks, including view integration (Tatler & Land, 2011), obstacle avoidance (Hardiess, Hansmann-Roth, & Mallot, 2013), spatial updating (Kelly, McNamara, Bodenheimer, Carr, & Rieser, 2008; Loomis, Klatzky, & Giudice, 2013), or spatial memory and recall (Byrne, Becker, & Burgess, 2007; Röhrich, Hardiess, & Mallot, 2014).

In this working memory stage, nonstereoscopic depth cues and more abstract shape information may also play a role in gauging ego-motion perception. One possible cue is eye height above ground, which can be assumed to be known or at least fixed. Indeed, Frenz and Lappe (2005) demonstrated that judgments of traveled distances above a ground plane depend linearly on simulated distance with a scaling factor

close to eye height. Familiar object size is another possible cue to depth, which has been demonstrated to play a role in velocity constancy observed when subjects judge the relative velocity of objects moving at different distances from the observer (e.g., Distler, Gegenfurtner, Veen, & Hawken, 2000; Martin, Chambeaud, & Barraza, 2015). It therefore seems possible that the size of familiar objects is used not only to judge object velocities but also to assess ego-motion speed. Indeed, Buchner, Brandt, Bell, and Weise (2006) demonstrated that car drivers can judge the distance and time to collision with the car ahead from size familiarity cues such as back-light separation or the elevation of the back lights above street level. In Experiment 3, we used passages through alleys of blocks whose average size was kept constant along the way. Corridor narrowing and widening might therefore also be judged from the average visual angle subtended by each block at the beginning and the end of the passage.

In this article we study the interaction of optic flow and stereoscopic depth cues (both random dot and object based) in the perception of ego-acceleration. Ego-acceleration is an important variable in the control of movement because it can be used to stabilize ego-motion by a simple feedback loop. Ego-acceleration can be perceived from optic flow but suffers from a perceptual confusion similar to the depth–velocity ambiguity, which may be called a narrowing–acceleration confusion (Festl, Recktenwald, Yuan, & Mallot, 2012): Subjects confuse the narrowing of a tunnel with ego-acceleration and the widening of a tunnel with ego-deceleration.

Unlike the depth–velocity ambiguity, the narrowing–acceleration confusion is not a computational necessity because veridical judgments at least of the sign of ego-acceleration from optical flow are theoretically possible. This is why we call it a *confusion* rather than an *ambiguity* in this article. To see this, consider an observer moving along the z-axis of the camera coordinate system with a time course $z(t)$. Time to collision is defined as $\tau = z/\dot{z}$, where $\dot{z}$ is the temporal derivative of z (i.e., the current ego-motion speed). Time-to-collision measurements can be made on retinal data at any time. Now consider two time-to-collision (or time-to-passage) measurements carried out for the same target at times t_1 and t_2. If the observer is moving at a constant speed, the second measurement should be reduced with respect to the first by the amount $\tau(t_2) - \tau(t_1) = -(t_2 - t_1)$, which implies $\dot{\tau}(t) = -1$ (cf. Lee, 1980). If $\dot{\tau}$ differs from -1, ego-motion has undergone acceleration or deceleration. $\dot{\tau}$ is related to the acceleration rate $\rho = \ddot{z}/\dot{z}$, defined by Festl et al. (2012) by the relation $\rho = (1 - \dot{\tau})/\tau$. Note that the use of ρ allows quantitative estimates of ego-acceleration, not just its sign.

The use of $\dot{\tau}$ for the control of braking was suggested by Lee (1980) and has been tested experimentally—for example, by Rock, Harris, and Yates (2006) and Yilmaz and Warren (1995). While braking behavior may indeed produce a constant $\dot{\tau}$ of $-1/2$, as predicted by Lee (1980), the same behavior may also result from other strategies not explicitly using $\dot{\tau}$, such as calculating the deceleration needed to stop at a given point (Rock et al., 2006). This finding is in line with the result of Festl et al. (2012) that acceleration rate ρ, a close relative of $\dot{\tau}$, is ignored in ego-acceleration detection.

In this article we study the perception of ego-acceleration from optic flow and stereoscopic cues. We designed three experiments to test the role of optic flow and stereoscopic depth cues in the judgment of ego-motion (Experiments 1 and 3) and in the stabilization of the ego-motion speed (Experiment 2). Experiment 1 was a repetition of the Festl et al. (2012) experiment with veridical stereo disparities. Experiment 2 addressed the same question with an adjustment task in which subjects were asked to keep constant ego-motion speed in a tunnel with varying diameter. Because stereo perception from dynamic, limited lifetime random dots may be weak, we performed a third experiment with three-dimensional rendered objects placed along narrowing, straight, or widening streets. In this case, depth information may be provided by stereopsis, occlusion, constant average object size, and visual field elevation of the simulated objects.

Experiment 1: Thresholds for perceived ego-acceleration

The purpose of this experiment was to test the hypothesis that the confusion of corridor narrowing and ego-acceleration reported by Festl et al. (2012) might be overcome by stereoscopic presentation of the stimulus providing independent structural information about the simulated environment.

Participants

Three male and three female participants, aged 19 to 36 years, took part in the experiment. All participants had normal or corrected-to-normal vision and were able to see stereoscopic depth and stereoscopically defined shapes in random dot stereograms taken from Julesz (1971). Before the experiment started, participants were informed about the experimental procedure and their right to terminate participation at any time. All participants gave their written informed consent.

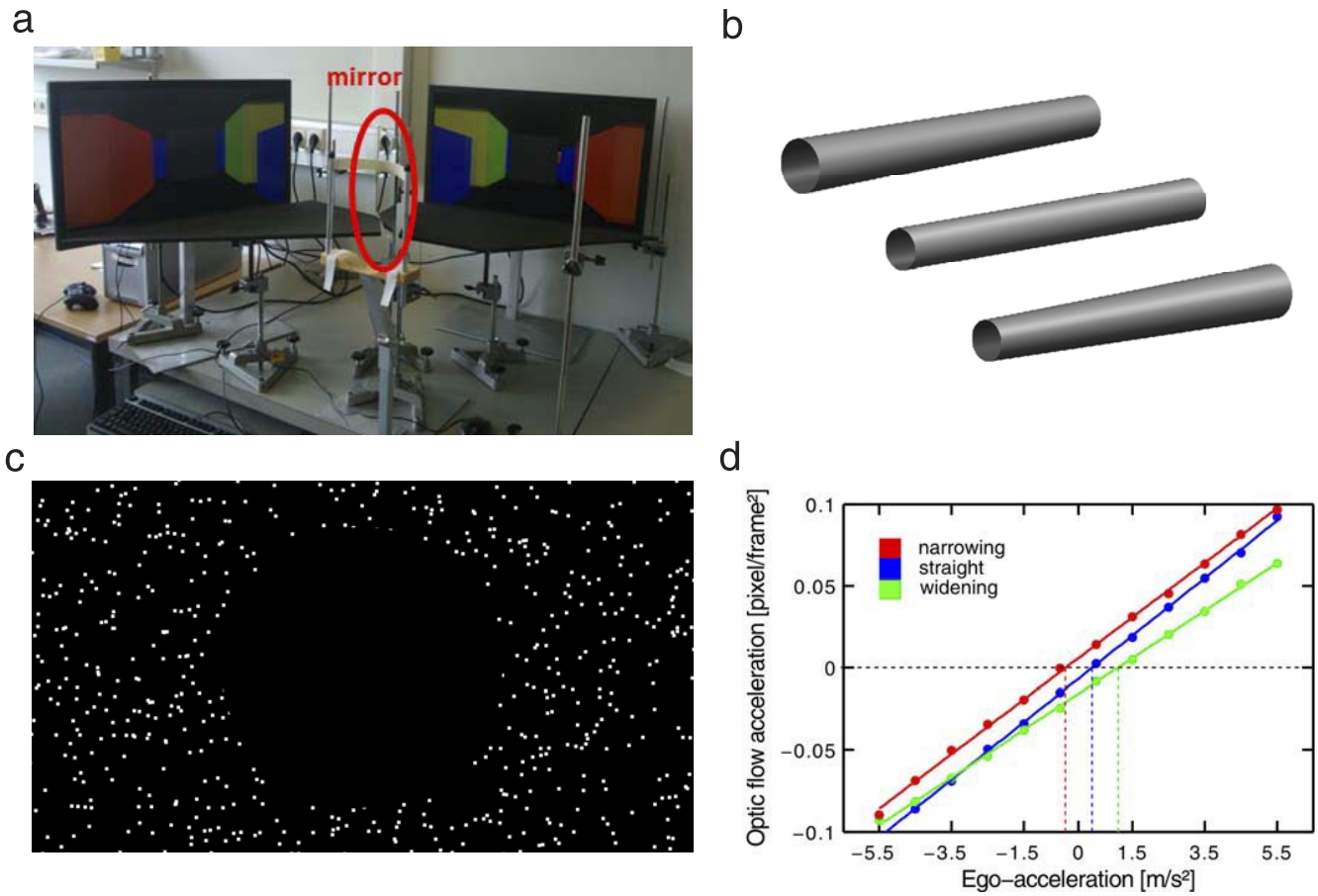

Figure 1. Setup and stimuli. (a) Single-mirror stereoscope. The two half-images of a stereogram appear on two 27-in. liquid crystal display monitors. The right one is viewed directly, whereas the left one is viewed via a mirror (appearing in the image behind the chin rest). Note that the left half-image is left–right inverted to compensate for this mirroring. The scene appearing on the monitors depicts a stimulus from Experiment 3. (b) Tunnel shapes (narrowing, straight, and widening) used in Experiment 1. The travel length in each tunnel is 30.3 m. (c) Screenshot of the stimulus of Experiment 1. Note that the central black disk is the occluder moving in front of the subject, not the end of the tunnel. Dots have been enlarged for better visibility. (d) Translational optic flow of the presented stimuli. The relative shift of the lines reflects the fact that optic flow speeds up faster in the narrowing corridor. The dashed colored lines mark the theoretical PSC, which are derived by reading the simulated ego-acceleration for which optic flow acceleration is zero. 1 pixel/frame^2 = 56.5°/s^2.

Apparatus

The stereoscope used in this and the following experiments is illustrated in Figure 1a. It consisted of two calibrated 27-in. high-resolution computer screens (S27A850D, Samsung, Suwon, South Korea; frequency = 60 Hz; resolution = 2560 × 1440 pixels). To enable stereoscopic vision, one frontally positioned screen displayed the right stereo half-image directly to the right eye. The left stereo half-image appeared on the second screen placed on the left side of the observer; this screen was viewed through a mirror placed in front of the subject such that the right eye's view was not affected (single-mirror stereoscope; see Kollin & Hollander, 2007). Viewing distance to the screens was 80 cm, which amounts to a visual angle of 40.2° horizontally and 24° vertically. Subjects were comfortably seated in a chair with their head placed in a chin rest to ensure stable head position. Room light was dimmed to a mesopic condition. To further reduce disturbances due to scattered light during the procedure, the whole stereoscopic system and the subjects' eyes were shielded from ambient light by a black box. In the monocular presentation condition, the sight of one eye was blocked by an occluder.

Stimuli

Three-dimensional visual environments were tubular or conic tunnels with linearly changing diameter. Three shapes were used: a narrowing tunnel (diameter of 4.14 to 3.14 m from start to stop, corresponding to a narrowing of 24%), a straight tunnel (constant diameter

of 3.14 m), and a widening tunnel (diameter varying from 3.14 to 4.14 m, corresponding to a widening of 32%). Travel length in the tunnel was 30.3 m for all conditions. The tunnels extended with constant conic angle somewhat beyond the end position at 30.3 m. A circular black occluder covering a diameter of 20° of visual angle was moving at a fixed distance in front of the subject at all times. Together with the tunnel extension, this occluder ensured that the end of the tunnel was never visible. This is important because the diameter of the tunnel ending is different in the three shape conditions and might provide a confounding cue to the subjects. The disparities occurring during the stereo condition vary with narrowing condition and image position. As an example, consider a situation in which the subject is fixating a dot just outside the occluder in the straight tunnel. A second point appearing 1° of visual angle farther out will then have a relative disparity of −2.5 minutes of arc.

Subjects were free to make eye movements, and eye movements were not recorded. Optic flow–related eye-movement sequences have been shown to consist of pursuit episodes directed to individual moving dots in a stimulus field extending ±20° horizontally and +5° to 20° vertically (Lappe & Hoffmann, 2000). Using free viewing and combined head and eye tracking, Hardiess et al. (2013) showed that moving targets on the horizontal midline are tracked at eccentricities of up to ±120° with respect to heading. Tracking of individual points is also what our subjects reported to do in the debriefings. We therefore assume that stereo disparities were observed foveally even though the central part of the screen (i.e., the part in heading direction) was empty. Even if a subject would look directly into the (empty) center of the occluder, the disparity of the least eccentric dots (eccentricity = 10°) would still be in the order of the stereo threshold for this eccentricity, which was reported to be between 1 and 3 minutes of arc by Siderov and Harwerth (1995) and Wardle, Bex, Cass, and Alais (2012).

Environments were modeled with MultiGen Creator software (Version 5.2.1; www.presagis.com) and rendered with a self-written software generating stereoscopic random dots with limited lifetime and homogeneous density on the screen. Dot size was set to 5 pixels, and dot lifetime varied randomly between 16 and 1000 ms. When a dot reached the end of its lifetime or left the field of view, a new stereoscopic pair of dots was generated at a random position on the screen, with the disparity defined by the local depth of the environment. About 1,150 dots were displayed on the screen at any one frame. The experimental software was installed on an Intel Core i5 computer (3-Gb random-access memory) with an enhanced graphics processing unit (GeForce GTX 570, NVIDIA, Santa Clara, CA).

Stimuli were flights through the tunnels lasting for 3 s each (i.e., with a fixed average speed of 10.1 m/s). Simulated ego-motion profiles of the form $z(t) = v_o t + at^2/2$ were calculated for 12 ego-acceleration conditions where acceleration a ranged from −5.5 to +5.5 ms^{-2} in steps of 1 ms^{-2}. The initial velocity v_o was adjusted such that the fixed average velocity was obtained.

Stimuli were presented in either stereoscopic or monocular viewing. Stereo images were calculated with an interocular separation of 6.5 cm, fixed for all subjects. For the monocular presentation, the subdominant eye of the subject was determined with a simple pointing task. With both eyes open, subjects were asked to point their index finger to a distant target. Without changing the finger position, the subjects then alternately opened and closed one eye. The subdominant eye is the one in which the target appears farther away from the fingertip (cf. Kommerell, Schmitt, Kromeier, & Bach, 2003). The view of this eye was then blocked with an occluder. All experiments were performed in the stereoscope setup described above.

Procedure

Three independent factors were varied: viewing condition (mono, stereo), corridor shape (straight, narrowing, widening), and simulated ego-acceleration (12 levels). All conditions were tested in a within-subject design. In each trial, subjects were presented with a flight sequence and were required to decide whether they perceived an ego-acceleration (yes/no task). Note that the answer *no* includes all cases in which ego-deceleration or no change of ego-motion speed were perceived. The factor "viewing" was blocked in two separate sessions—that is, all monocular tasks were carried out first. If subjects saw the vivid depth simulations of the stereoscopic display before the monocular condition, they might be biased to more thoroughly search for remaining depth cues in the monocular displays (motion parallax). If this were the case, the expected differences between the two viewing conditions would have been reduced. The trials for the various tunnel shapes and ego-accelerations were presented in pseudorandom sequence. For each corridor shape and subject, a total of 306 choice trials were carried out in three sessions. Sessions 1 and 2 followed the method of fixed stimuli with 10 trials per ego-acceleration value. After Session 2, a preliminary psychometric function fit was calculated. In Session 3, 60 trials in the vicinity of the threshold (±3 ego-acceleration steps) were mixed with 36 trials again from a constant stimuli scheme.

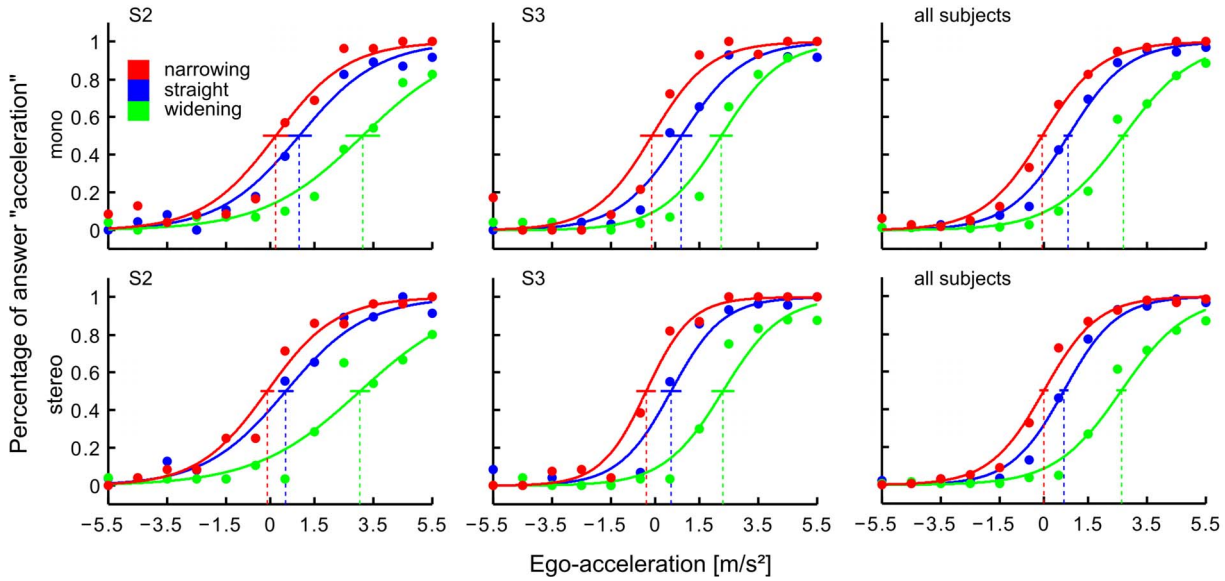

Figure 2. Psychometric functions from Experiment 1 for two subjects (S2 and S3) and pooled over all six subjects (rightmost panels). Top: monocular presentation. Bottom: stereoscopic presentation. Dashed vertical lines mark the PSC. Horizontal lines at 50% correct are 95% confidence intervals.

Data analysis

Data analysis was performed using MATLAB with the psychophysics toolbox Palamedes (Prins & Kingdom, 2009). Psychometric functions were fitted in the maximum likelihood sense with the logistic function

$$\Psi(x; a, \beta) := (1 + \exp\{-\beta(x - \alpha)\})^{-1}, \quad (1)$$

where α controls threshold and β slope. Standard deviations for α and β were determined by a bootstrap procedure provided by the toolbox. From these, 95% confidence intervals were calculated by multiplication with a factor of 1.96—that is, with the 95% two-sided fractile of the standard normal distribution (Kingdom & Prins, 2010). These confidence intervals for the α parameter are shown as horizontal bars in the psychometric functions of Figure 2. The α values themselves—that is, the points of subjective flow constancy (PSC)—are marked by dashed vertical lines in Figure 2.

Theoretical predictions for the PSC shifts in the three tunnel conditions were derived from the template-matching algorithm discussed by Festl et al. (2012). It assumes that the current flow field $\vec{v}(\vec{x},\ t)$ is matched to a fixed template $\vec{T}(\vec{x})$ by the equation $f_{tot}(t) := 1/|V| \int_V \vec{v}(\vec{x},\ t)\vec{T}(\vec{x})d\vec{x}$, where $\vec{x} = (x_1, x_2)$ denotes the image coordinates; $f_{tot}(t)$ is the total optic flow at time t; V and $|V|$ are the visual field and its area, respectively; and the multiplication under the integral is to be understood as a dot product. The template does not contain depth information, which is assumed unknown in the template algorithm. For forward translation, we therefore choose the template as $T(\vec{x}) = \vec{x}/||\vec{x}||$, for all $\vec{x} \neq 0$—that is, a radial pattern where all vectors have unit length. From actual videos of the flights through, we calculated time-dependent optic flow fields simply by taking the position difference of each dot in two subsequent frames. Dots leaving the visual field or reaching their lifetime limit were excluded from this analysis. The resulting flow field was matched to the template of radial flow vectors of constant length using the above equation. The result is a time-dependent number $f_{tot}(t)$, which was considered the optic flow estimate at each time frame. From these, optic flow acceleration was calculated as the slope of a linear regression line over all time steps of a flight—that is, by minimizing $\int(f_o + a_f t - f_{tot}(t))^2 dt$ subject to a_f. This variable a_f is called the *optic flow acceleration* and is plotted in Figure 1d. For the straight corridor, optic flow acceleration is a linear function of simulated acceleration. For the narrowing corridor, acceleration is overestimated by an almost constant amount. The curve for the widening tunnel surprisingly leads to overestimation of acceleration in the negative acceleration range, whereas large accelerations are underestimated, as is to be expected. These curves are not a result of erroneous stimulus construction but have been confirmed in an analytical calculation. They indicate that the stimulus conditions of narrowing and widening are not as symmetric as they might appear. Finally, predicted PSC values are calculated by reverse evaluation of the acceleration function for optic flow acceleration zero, as indicated by the dashed lines in Figure 1d.

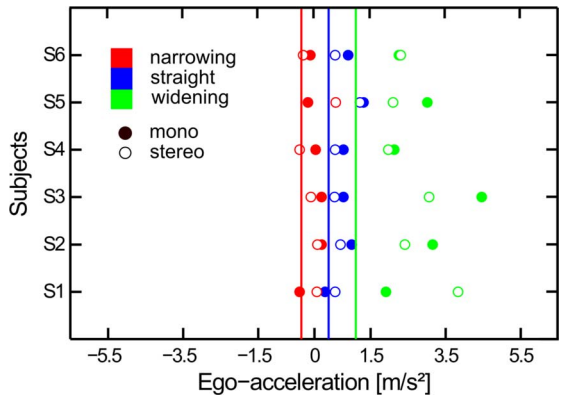

Figure 3. PSC for six subjects in the mono (filled symbols) and stereo (open symbols) conditions. The straight lines show theoretical PSC values derived from the theoretical optic flow accelerations shown in Figure 1d.

Results and discussion

Figure 2 shows sample results from two subjects and average results from a group of six subjects. Psychometric curves for the straight tunnel appear in the middle. With respect to these, the curves for narrowing and widening tunnels are shifted left and right, respectively, indicating that ego-acceleration is perceived for lower simulated accelerations in the narrowing tunnel and for larger simulated accelerations in the widening tunnel. This effect holds for both stereoscopic and monocular presentation. Horizontal bars are confidence intervals for the PSC values. PSC confidence intervals for the three shape conditions are nonoverlapping for both the stereoscopic and monocular viewing conditions, indicating significance on the 1% level. Note that the PSC confidence intervals are clearly overlapping when comparing stereoscopic and monocular presentation for any of the three shape conditions, indicating that the PSC shifts do not differ across viewing conditions.

The PSC values for all subjects appear in Figure 3 for monocular (filled symbols) and binocular (open symbols) viewing. All subjects show that the PSC shifts to the left for the narrowing corridor and to the right for the widening corridor. The solid lines mark the predicted PSC values derived from Figure 1d. They reproduce the direction of the PSC shifts and, at least for the narrowing and straight tunnels, the rough amount of PSC shift. For the widening corridor, large interindividual differences are found. Note that standard optic flow algorithms recovering jointly ego-motion and object nearness would predict veridical results (i.e., zero PSC shifts).

The results indicate that stereo cues provided in the experiments are not used in the disambiguation of spatial nearness and speed of retinal flow in ego-motion perception. The result is in fair quantitative agreement with the prediction of a simple template-matching algorithm, as was already shown in monocular or nonstereoscopic binocular stimulation by Festl et al. (2012).

The results for widening and narrowing corridors reported in Figure 3 show a marked asymmetry in the sense that the PSC shifts for widening corridors are larger than expected and differ substantially across subjects. This may be a simple consequence of the fact that the optic flow acceleration is related to the percentage of narrowing or widening relative to the entrance of the tunnel, which is of course different for the widening and narrowing tunnels. Another possible explanation of this effect can be given with respect to the theoretical curves for optical flow acceleration (Figure 1d) if we assume that the threshold for the "acceleration yes" response is not optical flow acceleration zero but rather a small positive value, depending on the subject. Because the theoretical curve of optic flow acceleration is least sloped for the widening conditions, this condition would be affected more. By the same token, noise added before the decision process would lead to larger variability for the widening condition than for the other conditions, as seems to be the case in Figure 3.

Stereoscopic depth information, although seemingly neglected in Experiment 1, might still play a role in other experimental settings—that is, if quantitative adjustment of perceived ego-motion speed is required or if stereo information is made more explicit by attaching it to solid objects rather than to dynamic random dots. These ideas are tested in the following experiments.

Experiment 2: Adjustment

The purpose of this experiment was to test the hypothesis that the confusion of corridor narrowing and ego-acceleration is not just a perceptual effect but rather enters the control mechanism of ego-motion speed. If this is true, we predict that subjects instructed to actively keep a constant speed slow down in a narrowing corridor and speed up in a widening corridor. The amount of slowing down or speeding up should depend on the slope of tunnel diameter, averaged over the current field of view. In order to provide for a reasonable range of diameter changes, we used sinusoidal diameter variations with various modulation amplitudes and frequencies. The logic of the experiment is inspired by the study of Snowdon, Stimpson, and Ruddle (1998), in which subjects were instructed to keep a constant speed while visibility of the environment decreased due to simulated fog.

Figure 4. Tunnel shape (modulated radius) used in Experiment 2. The total length of this tunnel is 1147 m, but different lengths were also used (see text). For better visibility, the radius is exaggerated by a factor of 3.

Participants

Six male and five female participants aged 21 to 29 years (22.7 ± 2.2 years) were recruited among the students of the University of Tübingen. All participants had normal or corrected-to-normal vision. All subjects were able to see stereoscopic depth and stereoscopically defined shapes in random dot stereograms taken from Julesz (1971). Before the experiment started, participants were informed about the experimental procedure and their right to terminate participation at any time. All participants gave their written informed consent.

Apparatus and stimuli

The experiment was carried out in the same stereoscopic setup described for Experiment 1. Stimuli were flights through cylindrical tunnels whose radius was sinusoidally modulated along tunnel length according to the following formula:

$$r(z) = \begin{cases} r_{\min} + A & \text{for} \quad z \le 100 \\ r_{\min} + A(1 + \sin(\omega z)) & \text{for} \quad 100 < z \le 100 + 10\pi/\omega, \end{cases} \tag{2}$$

where z is length along the tunnel and $r_{\min}$ was set to 1.5 m. Modulation amplitude A and frequency ω were modulated in two separate conditions as $A = 1.0$, 1.5, and 2.0 m and $\omega = 0.02$, 0.03, and 0.04/m, resulting in the wavelengths $\lambda = 2\pi/\omega = 315$, 471, and 628 m.

Each tunnel comprised an initial cylindrical section of 100-m length with constant radius $r_{\min} + A$, followed by five complete cycles of the sinusoidal modulation, resulting in a total length of 100 m + 10 π/ω. An example tunnel with cylindrical initial section and five modulations is shown in Figure 4. Flights through were displayed by stereoscopic random dots with limited lifetime, varying at random between 40 and 80 ms. Throughout the flight, a total of 1,000 dots was visible on the screen. A circular black disc void of dots, subtending 8.2° of visual angle (diameter), was moving at constant distance in front of the subject, occluding the tunnel exit at all times. Eye separation for stereo display was set to 6.5 cm.

Procedure

Subjects were given a joystick to control simulated ego-motion speed. In the experimental session, subjects were instructed to keep their ego-motion velocity constant at all times. Initial velocity was set to 15 m/s (target velocity), and subjects were told to use the initial section of the corridor to get a feeling for this target velocity. Note that the modulation of the corridors was rather shallow so that no abrupt diameter changes or self-occlusions of the walls could be perceived. Velocity adjustments as a function of z position in the corridor were recorded as a dependent variable.

Prior to the test session, subjects were given a familiarization phase in which they traveled a tubular tunnel with a constant radius of 4.5 m and a length of 500 m to explore the handling of the joystick. The tubular tunnel was also used intermittently during the test phase to remind the subjects of the target velocity.

In the amplitudes condition, the spatial frequency parameter of the tunnels was fixed to $\omega = 0.03$/m. Three tunnels for each of the amplitudes $A = 1.0$, 1.5, and 2.0 m (i.e., a total of nine tunnels) were concatenated in a fixed random sequence, with a tubular section between each two. In addition, in the middle of the whole sequence, we added a distractor tunnel with modulation amplitude changing after each completed cycle (six cycles with amplitudes 2.0, 1.5, 1.0, 1.5, 1.0, and 2.0). The overall random sequence was $T - A_{1.0} - T - A_{1.5} - T - A_{2.0} - T - A_{1.5} - T - A_{2.0}$ – distractor – $T - A_{1.0} - T - A_{2.0} - T - A_{1.0} - T - A_{1.5}$, where T denotes the tubular tunnel and $A_{1.0}$ denotes the modulated tunnel with $A =$ 1.0 m and so on.

In the frequencies condition, the amplitude parameter in Equation 2 was fixed to $A = 3.0$ m in all cases. Three tunnels for each of the spatial frequency settings $\omega = 0.02$, 0.03, and 0.04/m (i.e., a total of nine tunnels) were concatenated in a fixed random sequence, with a tubular section between each two. Note that the length of the individual tunnels varies with frequency because five full cycles were included in each tunnel. The overall test sequence was $T - F_{.02} - T - F_{.03} - T - F_{.04} - T - F_{.03} - T - F_{.04} - T - F_{.02} - T - F_{.04} - T - F_{.02} - T - F_{.03}$, where T denote the tubular tunnel and $F_{.02}$ denotes the modulated tunnel with frequency parameter $\omega = 0.02$/m and so on.

After the familiarization task, the test took about 30 min to complete. Five subjects were assigned to the amplitude condition, and six subjects were assigned to the frequency condition.

Data analysis

The velocity adjustments produced in the tunnel sections with sinusoidal width modulation with a given

frequency ω were fitted using a sinusoidal with that same frequency,

$$v(z) = A^* \sin(\omega z - \phi^*), \quad (3)$$

using a simple least-squares procedure. A^* and ϕ^* are free parameters of the fit. Because the tunnels were repeated three times in the experimental procedure, three amplitude and phase estimates were obtained per subject for each amplitude and frequency condition. Theoretical optical flow amplitude was calculated from the actual random dot displays using the procedure described also for Experiment 1 and presented in Figure 5b.

Results and discussion

Figure 5 summarizes the procedure of Experiment 2. The two columns (left and right) correspond to the amplitude and frequency conditions. The top row shows the width modulation of the used test tunnels along the first 500 m. The second row shows the calculated radial flow components of the stimuli. The deviations from sinusoidal shape, especially for the narrower tunnels, result from effects of visibility and perspective. The third row shows example traces of adjusted velocity from one subject. Note that the velocity modulation depends on the amplitude and frequency of width modulation. The last row shows the sinusoidal fits to the adjusted velocities.

Figure 6 shows the fitted amplitude values A^* and phase shifts ϕ^* (in degrees) for the amplitude and frequency conditions. The results show that velocity modulation increases with width modulation (Figure 6a), analysis of variance (ANOVA) $F(2, 22) = 34.91$, $p < 0.001$, $\eta_p^2 = 0.76$, on a roughly linear pace but decreases slightly with frequency (Figure 6b), ANOVA $F(2, 28) = 11.09$, $p < 0.001$, $\eta_p^2 = 0.44$. Phase shift is constant in the amplitude modulation condition, ANOVA $F(2, 22) = 2.84$, $p = 0.08$, $\eta_p^2 = 0.21$ (see Figure 6c) but shows an unexpected v-shaped dependence on frequency, ANOVA $F(2, 28) = 28.74$, $p < 0.001$, $\eta_p^2 = 0.67$ (see Figure 6d).

The increase of the amplitude of velocity modulation (Figure 6a) with the amplitude of tunnel width modulation is well in line with the template-matching model for the detection of ego-motion speed. The slight decrease with increasing frequency of tunnel modulation may be due to the fact that the subject is overlooking a section of the tunnel of roughly equal length in all conditions and phases of the experiment. This section, however, shows more diameter modulation in the higher frequency conditions. Because the template-matching algorithm involves an averaging over the entire visual field, it generates a low-pass effect, which may account for the present result. Phase shifts between the diameter modulation and the velocity modulation in the adjustments are probably due to the same effect, which however does not explain the v-shaped dependence on modulation frequency shown in Figure 6d. Note that traveling one cycle of the diameter modulation takes about 10 s, which probably rules out perceptual delays as a source of phase shift in our data.

In summary, the data indicate that the confusion of ego-acceleration and tunnel narrowing is not just a perceptual effect of acceleration versus deceleration judgments but rather affects also the control of ego-motion speed in an adjustment task.

Experiment 3: Object-based motion

The purpose of this experiment was to test the confusion of ego-acceleration and tunnel narrowing in a block-world environment consisting of two rows of blocks aligned along the margins of a street. Thus, the perception of depth and image motion could be based not just on limited lifetime random dots but also on stereoscopic disparities of solid objects, mutual occlusion of such objects, and perspective. The size of the objects varied around a fixed average such that changes in corridor width might also be judged by changes in the average visual angle subtended by the objects.

Participants

Six male participants and one female participant, aged 20 to 28 years, were recruited among the students of the University of Tübingen. All participants had normal or corrected-to-normal vision and were able to see stereoscopic depth as well as stereoscopically defined shapes in random dot stereograms taken from Julesz (1971). Before the experiment started, participants were informed about the experimental procedure and their right to terminate participation at any time. All participants gave their written informed consent.

Apparatus and stimuli

The experiment was carried out with the stereoscopic setup used also for the other experiments (Figure 1a). Environments were simulated streets or alleys passing through an arrangement of blocks (see Figure 7). Block sizes varied from 0.4 to 1.1 m (elevation) and from 0.7 to 2.0 m (width and length). Blocks had one of three possible colors (red, blue, or green) and were rendered with Lambertian shading. Eighteen blocks were placed with variable separation (1–2 m) along both sides of a

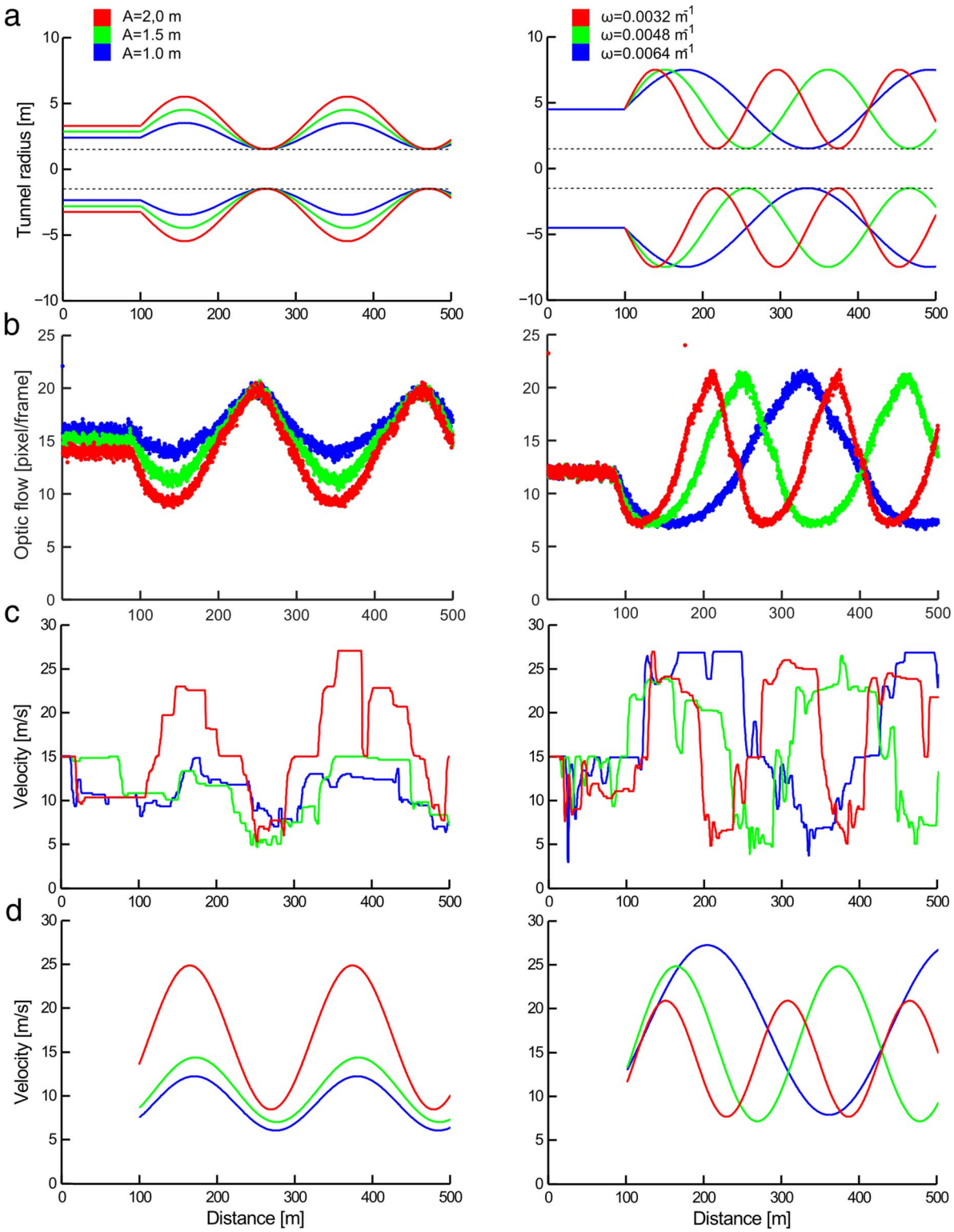

Figure 5. Experiment 2: stimuli and data analysis. Left column: amplitudes condition; right column: frequencies condition. Only the first 500 m of each tunnel is shown. (a) Tunnel shape. (b) Theoretical estimate of optic flow presented at each position. (c) Adjusted velocities (sample data from one subject). (d) Sinusoidals fitted to the adjusted velocity curves appearing in panel c.

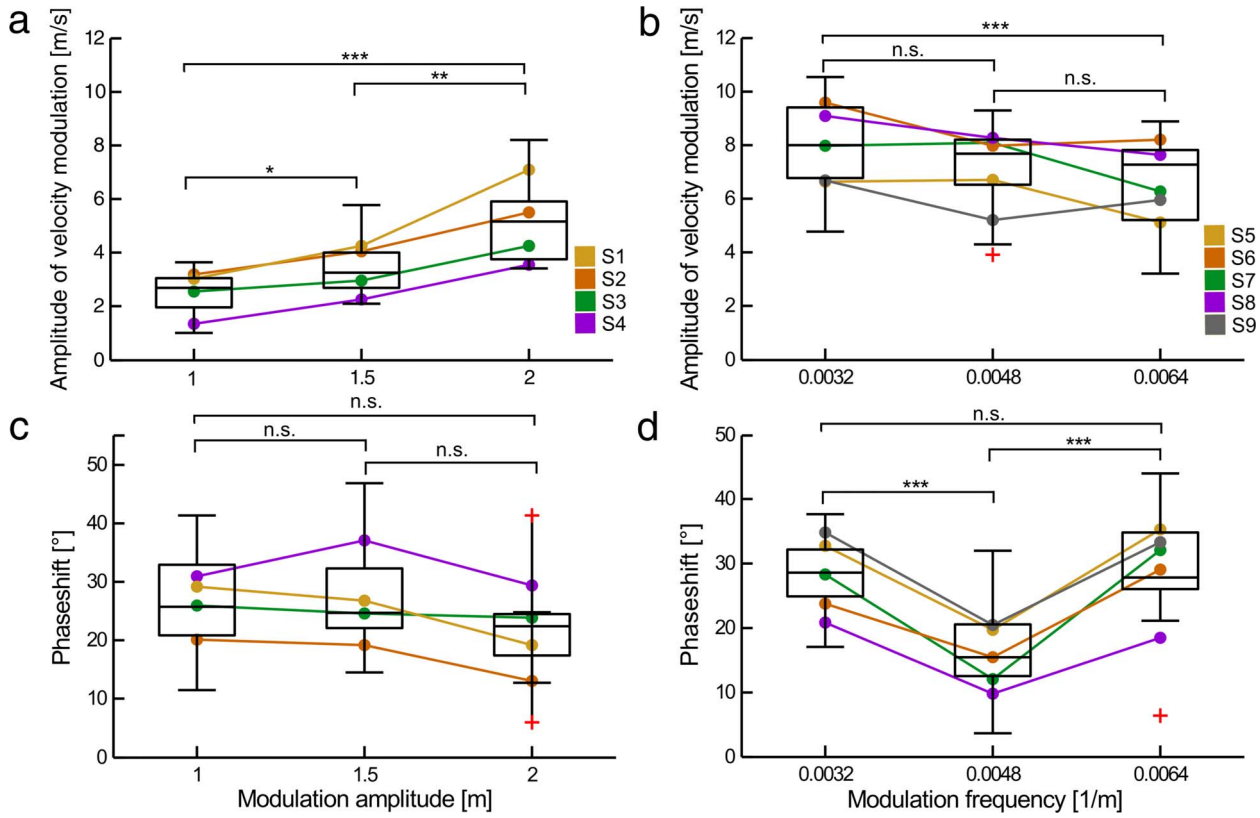

Figure 6. Results of Experiment 2. (a, c) Amplitude modulation. (b, d) Frequency modulation. (a, b) Amplitude of sinusoidals fitted to the adjusted velocities. (c, d) Phase shift of sinusoidals fitted to the adjusted velocities. Box plots show the distributions of the values over all subjects and trials; colored dots and lines show average values for the individual subjects. Significances refer to post hoc *t* tests (n.s. = not significant; *$p < 0.05$; **$p < 0.01$; ***$p < 0.001$).

street, where the margin of the street was defined by the block frontal faces. As in Experiment 1, three street shapes were used, all with 2-m width at the start position. In the straight, narrowing, and widening conditions, street width was constant, narrowed to 1.5 m, or widened to 2.5 m, respectively, at a travel distance of 30 m. For each of the three conditions, 10 block arrangements satisfying the above specifications

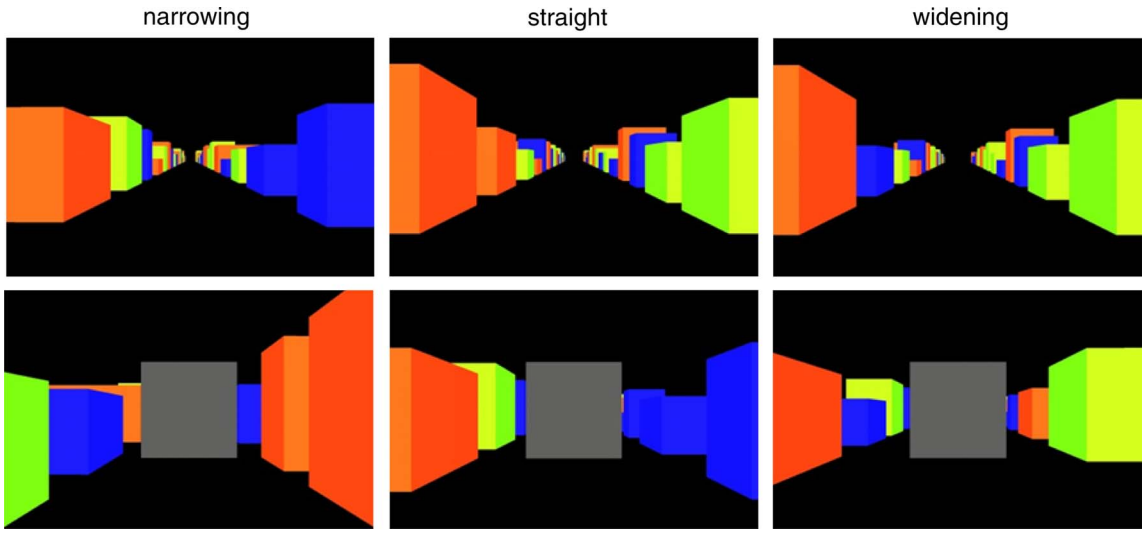

Figure 7. Sample scenes from stimuli of Experiment 3. Top row: View of the block world along the three street types. Bottom row: Actual stimulus with gray occluder moving in front of the subject.

were generated at random and assigned randomly to the test trials.

In the actual experiments, a gray square occluder covering the central 12° × 12° of the visual field moved at a constant distance of 1.9 m in front of the subject to prevent inspection of the far end of the alley, which would otherwise provide a cue to corridor shape (bottom row of Figure 7). As in Experiment 1, stimuli were drives through the initial 30-m segment of the alleys, lasting for 3 s each (180 image frames), resulting in an average speed of 10 m/s. Simulated ego-motion profiles of the form $z = vt + at^2/2$ were calculated for 12 ego-acceleration conditions, where acceleration a ranged from −5.5 to +5.5 m s^{-2} in steps of 1 m s^{-2}. The initial velocity was adjusted such that constant average velocity was obtained. Interocular separation was set to 6.5 cm.

Procedure and data analysis

Two independent factors were varied in the experiment: street shape (straight, narrowing, widening) and simulated ego-acceleration (12 levels). All conditions were tested in a within-subject design. In each trial, subjects were presented with a drive-through sequence and were required to decide whether they perceived an ego-acceleration (forced-choice yes/no task). Twenty repetitions were carried out for each street shape and acceleration, resulting in a total of 720 trials ($3 \times 12 \times 20 = 720$), which were carried out in random sequence (method of fixed stimuli). The experiment took 40 to 60 min to complete. Data analysis was as in Experiment 1.

Results and discussion

Figure 8 shows results from two sample subjects and average results from the group of all seven subjects. The center (blue) curve shows data for the straight street. The curves for the narrowing (red) and widening (green) streets show the same pattern of displacement as already found in Experiment 1. PSC and confidence intervals are also marked in the figure. The results show that the narrowing–acceleration confusion persists even in the stereoscopic block-world environment. The PSC offsets are smaller than in Experiment 1. However, theoretical estimates for expected PSC shifts in the block-world case require assumptions about the contrast dependence of motion detection and are therefore omitted.

General discussion and conclusions

In this article, we present three experiments on the perception of ego-acceleration from visual cues. The results indicate that the perception of ego-acceleration in environments with changing distance scale is not veridical, even if independent stereoscopic information to environmental depth is available. Rather, the confusion of ego-acceleration and scale reduction (tunnel narrowing) or ego-deceleration and scale increase (tunnel widening) that was observed for nonstereoscopic viewing by Festl et al. (2012) remains even with stereoscopic presentation. It is not restricted to the detection of ego-acceleration (Experiments 1 and 3) but rather also occurs in an adjustment task in which subjects were told to keep their perceived speed constant.

The neglect of information about environmental depth in ego-motion perception is not limited to stereoscopic depth information provided by dynamic random dots, which arguably form a rather weak depth cue. In Experiment 3, we used object-based depth information providing a variety of consistent depth cues such as stereo disparities, occlusion, and constant average object size, all of which are independent of optic flow. Still, the narrowing–acceleration confusion remains. The PSC shifts as shown in Figure 8 are slightly weaker than in Experiment 1, although the amount of tunnel or street narrowing is the same in both experiments (25%; 4.14 m to 3.14 m in Experiment 1 and 2.0 m to 1.5 m in Experiment 3). If the initial motion detection step is not affected by the different image contrasts and featural information available in the two experiments, an equal amount of optic flow increase should be required to compensate for the equal amounts of narrowing. The small PSC shifts in Experiment 3 might therefore indicate a reduced narrowing–acceleration confusion with object-based depth information. Object-based depth information might enter the process of ego-motion detection, whereas point-based stereo disparities do not. This possibility requires further investigation.

In all experiments we used an occluder, thus preventing the subjects from seeing the end of the tunnels or corridors. The reason for this was that the visual angle of the tunnel end differs in the different shape conditions and would therefore provide an unwanted cue to corridor shape. We think that stereo visibility was not affected by this occluder because (a) subjects were free to make eye movements and reported to fixate individual dots or objects during the experiment, (b) stereo disparities were large enough for peripheral stereo vision even if the gaze was directed into the center of the occluder, and (c) subjects reported to see stereoscopic depth. The occluder might also influence the results if the subjects erroneously take the occluder for the end of the tunnel and use this as a cue to tunnel shape. In this case, however, we would not expect to see the clear differences in PSC between the three shape conditions.

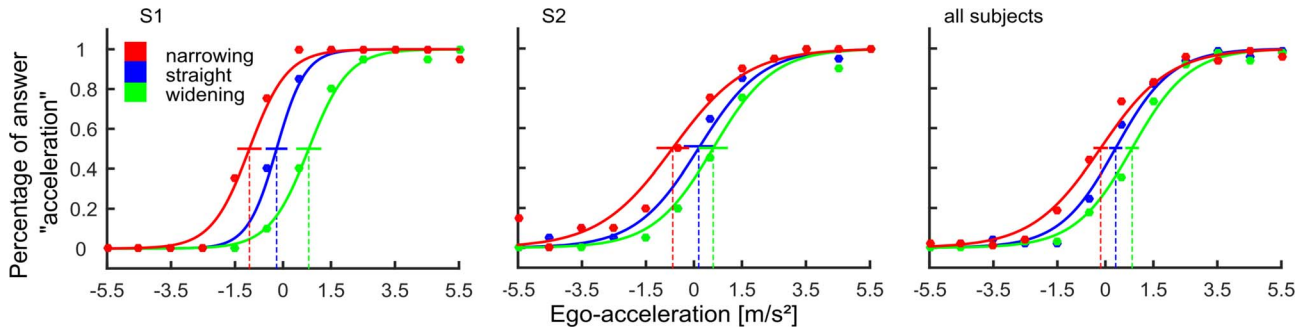

Figure 8. Psychometric function for two sample subjects and pooled over all seven subjects from Experiment 3. The effect persists even if optic flow is defined by three-dimensional blocks presented stereoscopically.

The list of depth cues used in this study clearly is not exhaustive, and we cannot exclude the possibility that other selections might have given different results. This is particularly true for the perception of speed constancy of distant objects, which we tried to account for by the constant average object size constraint used in the construction of the stimuli in Experiment 3. We have no independent evidence for this cue being recognized at all, but we can say that it was presented and did not lead to a resolution of the narrowing–acceleration confusion.

The findings reported in this article indicate that in the perception of ego-motion change, cues from optic flow and stereopsis are not combined on an early vision level, as would be possible in algorithms calculating object nearness as an intermediate stage for ego-motion from optic flow (Raudies & Neumann, 2012). This result confirms and extends earlier studies on the interaction of optic flow and stereopsis in ego-motion detection, which seem to indicate that interaction—if it occurs at all—is late (i.e., acts on extensively preprocessed data from initially separate streams). This view leaves open the possibility that higher level three-dimensional information, such as the object-based cues provided in Experiment 3, might be more efficient in reducing the narrowing–acceleration confusion than random dot–based stereo disparities. The interaction should then be seen more like the combination of representations in a common visual working memory (Kelly et al., 2008; Loomis et al., 2013) and not so much as the fusion of multimodal data in a joint early vision process.

Keywords: optic flow, stereopsis, cue integration, acceleration, ego-motion perception

Acknowledgments

This research was supported by the German Federal Ministry of Education and Research within the Tübingen Bernstein Center for Computational Neuroscience (Grant 01GQ1002A). We are grateful to Hansjürgen Dahmen for valuable discussions, to Till Becker and Matthias Hannig for help with the programming of the stimuli, and to Martina Schmöe-Selich for collecting part of the data.

Commercial relationships: none.
Corresponding author: Hanspeter A. Mallot.
Email: hanspeter.mallot@uni-tuebingen.de.
Address: Department of Biology, University of Tübingen, Tübingen, Germany.

References

Berthoz, A., Pavard, B., & Young, L. R. (1975). Perception of linear horizontal self-motion induced by peripheral vision (linearvection) basic characteristics and visual-vestibular interactions. *Experimental Brain Research, 23,* 471–489.

Brooks, K. R., & Rafat, M. E. (2015). Simulation of driving in low-visibility conditions: Does stereopsis improve speed perception? *Perception, 44,* 145–156.

Bruss, A. R., & Horn, B. K. P. (1983). Passive navigation. *Computer Vision, Graphics and Image Processing, 21,* 3–20.

Buchner, A., Brandt, M., Bell, R., & Weise, J. (2006). Car backlight position and fog density bias observer-car distance estimates and time-to-collision judgements. *Human Factors, 48,* 300–317.

Butler, J. S., Campos, J. L., Bülthoff, H. H., & Smith, S. T. (2011). The role of stereo vision in visual-vestibular integration. *Seeing and Perceiving, 24,* 453–470.

Byrne, P., Becker, S., & Burgess, N. (2007). Remembering the past and imagining the future: A neural model of spatial memory and imagery. *Psychological Review, 114,* 340–375.

Dichgans, J., & Brandt, T. (1978). Visual-vestibular

interaction: Effects of self-motion perception and postural control. In R. Held, H. W. Leibowitz, & H.-L. Teuber (Eds.), *Handbook of sensory physiology, Volume III, Perception* (pp. 755–804). Berlin, Germany: Springer Verlag.

Distler, H. K., Gegenfurtner, K. R., Veen, H. A. H., & Hawken, M. J. (2000). Velocity constancy in a virtual reality environment. *Perception, 29,* 1423–1435.

Ehrlich, S. M., Beck, D. M., Crowell, J. A., Freeman, T., & Banks, M. (1998). Depth information and perceived self-motion during simulated gaze rotations. *Vision Research, 38,* 3129–3145.

Festl, F., Recktenwald, F., Yuan, C., & Mallot, H. A. (2012). Detection of linear ego-acceleration from optic flow. *Journal of Vision, 12*(7):10, 1–12, doi:10.1167/12.7.10. [PubMed] [Article]

Franz, M. O., Chahl, J. S., & Krapp, H. G. (2004). Insect-inspired estimation of egomotion. *Neural Computation, 16,* 2245–2260.

Frenz, H., & Lappe, M. (2005). Absolute travel distance from optic flow. *Vision Research, 45,* 1679–1692.

Gray, R., & Regan, D. (1998). Accuracy of estimating time to collision using binocular and monocular information. *Vision Research, 38,* 499–512.

Gu, Y., Watkins, P. V., Angelaki, D. E., & DeAngelis, C. (2006). Visual and nonvisual contributions to three-dimensional heading selectivity in the medial superior temporal area. *The Journal of Neuroscience, 26,* 73–85.

Hardiess, G., Hansmann-Roth, S., & Mallot, H. A. (2013). Gaze movements and spatial working memory in collision avoidance: A traffic intersection task. *Frontiers in Behavioural Neuroscience, 7*(32), 1–13.

Harris, L. R., Jenkin, M., & Zikovitz, D. C. (2000). Visual and non-visual cues in the perception of linear self motion. *Experimental Brain Research, 135,* 12–21.

Heeger, D. J., & Jepson, A. D. (1992). Subspace methods for recovering rigid motion I: Algorithm and implementation. *International Journal of Computer Vision, 7,* 95–117.

Howard, I. P., Fujii, Y., & Allison, R. S. (2014). Interactions between cues to visual motion in depth. *Journal of Vision, 14*(2):14, 1–16, doi:10.1167/14.2.14. [PubMed] [Article]

Julesz, B. (1971). *Foundations of cyclopean perception*. Chicago, IL: Chicago University Press.

Kelly, J. W., McNamara, P. T., Bodenheimer, B., Carr, T. H., & Rieser, J. J. (2008). The shape of human navigation: How environmental geometry is used in maintenance of spatial orientation. *Cognition, 109,* 281–286.

Kingdom, F. A. A., & Prins, N. (2010). Psychophysics: A practical introduction. London, United Kingdom: Academic Press.

Koenderink, J. J., & van Doorn, A. J. (1987). Facts on optic flow. *Biological Cybernetics, 56,* 247–254.

Kollin, J., & Hollander, A. (2007). Re-engineering the Wheatstone stereoscope. *SPIE Newsroom,* doi:10.1117/2.1200703.0673.

Kommerell, G., Schmitt, C., Kromeier, M., & Bach, M. (2003). Ocular prevalence versus ocular dominance. *Vision Research, 43,* 1397–1403.

Lappe, M., & Hoffmann, K.-P. (2000). Optic flow and eye movements. *International Review of Neurobiology, 44,* 29–47.

Lappe, M., & Rauschecker, J. P. (1994). A neural network for the processing of optic flow from egomotion in man and higher mammals. *Neural Computation, 5,* 374–391.

Lee, D. N. (1980). Visuo-motor coordination in space-time. In G. E. Stelmach & J. Requin (Eds.), *Tutorials in motor behavior* (pp. 281–295). Amsterdam, The Netherlands: North-Holland.

Longuet-Higgins, H. C. (1981). A computer algorithm for reconstructing a scene from two projections. *Nature, 293,* 133–135.

Longuet-Higgins, H. C., & Prazdny, K. (1980). The interpretation of a moving retinal image. *Proceedings of the Royal Society London B, 208,* 385–397.

Loomis, J. M., Klatzky, R. L., & Giudice, N. A. (2013). Representing 3D space in working memory: Spatial images from vision, hearing, touch, and language. In S. Lacey & R. Lawson (Eds.), *Multisensory imagery: Theory and applications* (pp. 131–156). New York, NY: Springer.

Martin, A., Chambeaud, J. G., & Barraza, J. F. (2015). The effect of object familiarity on the perception of motion. *Journal of Experimental Psychology: Human Perception and Performance, 41,* 283–288.

Mohler, B. J., Thompson, W. B., Creem-Regehr, S. H., Pick, H., Jr., & Warren, W. H., Jr. (2007). Visual flow influences gait transition speed and preferred walking speed. *Experimental Brain Research, 181,* 221–228.

Palmisano, S. (1996). Perceiving self-motion in depth: The role of stereoscopic motion and changing-size cues. *Perception & Psychophysics, 58,* 1168–1176.

Palmisano, S. (2002). Consistent stereoscopic information increases the perceived speed of vection in depth. *Perception, 31,* 463–480.

Palmisano, S., Allison, R. S., Schira, M. M., & Barry, R. J. (2015). Future challenges for vection research: Definition, functional significance, measures, and neural bases. *Frontiers in Psychology, 6*(193), 1–15.

Perrone, J. A., & Stone, L. S. (1994). A model of self-motion estimation within primate extrastriate visual cortex. *Vision Research, 34,* 2917–2938.

Prins, N., & Kingdom, F. A. A. (2009). *Palamedes: Matlab routines for analysing psychophysical data*. Retrieved from www.palamedestoolbox.org

Raudies, F., & Neumann, H. (2012). A review and evaluation of methods estimating ego-motion. *Computer Vision and Image Understanding, 116,* 606–633.

Rieger, J. H., & Lawton, D. T. (1985). Processing differential image motion. *Journal of the Optical Society of America A, 2,* 354–360.

Rock, P. B., Harris, M. G., & Yates, T. (2006). A test of the tau-dot hypothesis of braking control in the real world. *Journal of Experimental Psychology: Human Perception and Performance, 32,* 1479–1484.

Röhrich, W., Hardiess, G., & Mallot, H. A. (2014). View-based organization and interplay of spatial working and longterm memories. *PLoS ONE, 9*(11), e112793.

Siderov, J., & Harwerth, R. S. (1995). Stereopsis, spatial frequency, and retinal eccentricity. *Vision Research, 35,* 2329–2337.

Snowdon, R. J., Stimpson, N., & Ruddle, R. A. (1998). Speed perception fogs up as visibility drops. *Nature, 392,* 450.

Tatler, B. W., & Land, M. F. (2011). Vision and the representation of the surroundings in spatial memory. *Philosophical Transaction of the Royal Society London B, 366,* 596–610.

van den Berg, A. V., & Brenner, E. (1994). Why two eyes are better than one for judgement of heading. *Nature, 371,* 700–702.

Wardle, S. G., Bex, P. J., Cass, J., & Alais, D. (2012). Stereocuity in the periphery is limited by internal noise. *Journal of Vision, 12*(6):12, 1–2, doi:10.1167/12.6.12. [PubMed] [Article]

Wist, E., Diener, H. C., Dichgans, J., & Brandt, T. (1975). Perceived distance and the perceived speed of self-motion: Linear vs. angular velocity? *Perception & Psychophysics, 17,* 549–554.

Yilmaz, E. H., & Warren, W. H., Jr. (1995). Visual control of braking. *Journal of Experimental Psychology: Human Perception and Performance, 21,* 996–1014.